

Geophysical Research Letters

RESEARCH LETTER

10.1029/2021GL094293

Key Points:

- We quantify land water resources change in response to rising CO₂ for different wetness levels using a new wetting contrast index
- We find a substantial amplification of runoff contrast across wetness levels because the runoff increases more in wet than dry regions
- Vegetation responses to rising CO₂ contribute to amplified runoff contrast by suppressing evapotranspiration more in wet than dry regions

Supporting Information:

Supporting Information may be found in the online version of this article.

Correspondence to:

S. Piao and H. Yang,
slpiao@pku.edu.cn;
yang_hui@pku.edu.cn

Citation:


Cui, J., Yang, H., Huntingford, C., Kooperman, G. J., Lian, X., He, M., & Piao, S. (2021). Vegetation response to rising CO₂ amplifies contrasts in water resources between global wet and dry land areas. *Geophysical Research Letters*, 48, e2021GL094293. <https://doi.org/10.1029/2021GL094293>

Received 10 MAY 2021

Accepted 26 JUN 2021

© 2021. American Geophysical Union.
 All Rights Reserved.

Vegetation Response to Rising CO₂ Amplifies Contrasts in Water Resources Between Global Wet and Dry Land Areas

Jiangpeng Cui¹ , Hui Yang^{1,2} , Chris Huntingford³ , Gabriel J. Kooperman⁴ , Xu Lian¹, Mingzhu He¹, and Shilong Piao^{1,5,6} 

¹Sino-French Institute for Earth System Science, College of Urban and Environmental Sciences, Peking University, Beijing, China, ²Department of Biogeochemical Integration, Max Planck Institute for Biogeochemistry, Jena, Germany, ³Centre for Ecology and Hydrology, Wallingford, UK, ⁴Department of Geography, University of Georgia, Athens, GA, USA, ⁵Key Laboratory of Alpine Ecology and Biodiversity, Institute of Tibetan Plateau Research, Chinese Academy of Sciences, Beijing, China, ⁶Center for Excellence in Tibetan Earth Science, Chinese Academy of Sciences, Beijing, China

Abstract Rising atmospheric CO₂ impacts on vegetation physiological processes can alter land feedbacks on precipitation and water resources, but understanding of regional differences in these changes is uncertain. We investigate the impact of rising CO₂ on land water resources for different wetness levels using four Earth system models. We find an overall tendency of runoff to increase across all wetness levels. However, runoff increases in wet regions are much larger than those in dry regions, especially in wet seasons. This substantial amplification of contrasts between wet and dry regions increases at 3% per 100 ppm increase in CO₂ relative to the historical period, reaching 18% for a quadrupling of CO₂, quantified by a new wetting contrast index (WCI). Physiological effects suppress evapotranspiration more in wet than dry regions, which has a larger contribution than radiative forcing to the amplification of runoff contrast, reshaping the spatial distribution of future land water resources.

Plain Language Summary Increasing atmospheric CO₂ concentration is expected to intensify the global water cycle and reshape the regional distribution of water resources. Using specialized simulations from four Earth system models, this study shows that physiological effects (stomatal closure and leaf area increase), rather than radiative forcing, of rising CO₂ are the main driver of amplified regional wetness contrasts, with stronger suppression of evapotranspiration and so larger runoff increases in wet regions than in dry regions. These results underscore the importance of accounting for the physiological forcing of rising CO₂ in hydrological change projections, and imply the urgency for future water resource assessments and managements to adapt for an increasing imbalance in regional water resources.

1. Introduction

The global hydrological cycle is expected to experience major changes under rising atmospheric CO₂ concentrations, many of which will have strong spatial heterogeneity (Held & Soden, 2006; Chou et al., 2009; IPCC, 2013; Allan et al., 2020). One of the most prominent descriptions of a varying hydrological cycle offered by researchers is the “wet regions get wetter, dry regions get drier” (WWDD) paradigm (Chou et al., 2009; Held & Soden, 2006). Many studies have demonstrated that the WWDD concept has some applicability on global-scales (Chou et al., 2009; Held & Soden, 2006; Kumar et al., 2015; Liu & Allan, 2013; Polson & Hegerl, 2017; Seager & Vecchi, 2010; Trenberth, 2011) or for ocean areas (Durack et al., 2012). However, more detailed analyses are suggesting that its validity over land may be uncertain (Chadwick et al., 2013; Greve et al., 2014; Roderick et al., 2014; Byrne & O’Gorman, 2015; Mankin et al., 2019). While the direct atmospheric response (i.e., climate change) to rising atmospheric CO₂ has received significant attention, there remains much uncertainty in its impact on the terrestrial hydrological cycle (De Kauwe et al., 2013; Mankin et al., 2019; Piao et al., 2007), in part due to sparse observations (Trancoso et al., 2017; Ukkola et al., 2015; Yang et al., 2016) and low understanding of land-atmosphere couplings (Seneviratne et al., 2010). There is an urgent need for a systematic assessment of the geographical dependence of these effects across wet or

dry regions consistent and comparable to the WWDD framework. This lack of understanding hinders water resources planning in response to higher CO₂ concentrations and related climate change.

Rising CO₂ levels affect the terrestrial hydrological cycle by altering atmospheric radiative forcing (hereafter referred to as the RAD driver) (Held & Soden, 2006; IPCC, 2013), which drives global warming (“greenhouse effect”) and additionally modulates rainfall patterns and other related changes such as humidity and downwelling radiative fluxes. However, increasing CO₂ levels also have strong physiological and structural effects on plants (hereafter referred to as the PHY driver) (Ainsworth & Rogers, 2007; Cao et al., 2010; Field et al., 1995; Kooperman et al., 2018; Scheff et al., 2021). PHY effects include stomatal closure (Ainsworth & Long, 2005; Field et al., 1995) and increased plant productivity (“CO₂ fertilisation”) and leaf area index (LAI) (Cowling & Field, 2003; Piao et al., 2020; Zhu et al., 2016). Transpiration is reduced by stomatal closure at the leaf level (Morison & Gifford, 1983), but can be increased by the CO₂-induced growth and related LAI increase at the ecosystem level (Piao et al., 2007). Over the last two decades, the development of land surface models has increased the representation of plant physiology (such as stomatal conductance) and carbon cycling, and growing attention has been drawn to the importance of the direct and often opposing PHY controls on the terrestrial hydrological cycle (Gedney et al., 2006; Piao et al., 2007; Swann et al., 2016; Fowler et al., 2019; Y. Yang et al., 2019). In general, the primary focus of research so far has been on overall temporal changes, and related combined mechanisms driving changes in the global hydrological cycle in response to the rising CO₂ (Betts et al., 2007; Fowler et al., 2019; Kooperman et al., 2018; Lemordant et al., 2018; Milly & Dunne, 2016; Pu & Dickinson, 2014; Swann et al., 2016). Fewer studies focus on the specific role of plant responses in generating regional heterogeneity of hydrological changes especially along different wetness levels in the context of the WWDD paradigm. Yet creating more localized information is essential for designing effective climate adaptation strategies. Hence the primary objective of this study is to investigate, individually, the CO₂-forced PHY and RAD impacts on the spatial patterns of the evolving land hydrological cycle. We place a specific focus on deriving any divergent characteristics to wet or dry regions.

2. Materials and Methods

2.1. Models and Experiments

We use Earth System Model (ESM) simulations from the Climate Model Intercomparison Project Phase 5 (CMIP5; <https://esgf-node.llnl.gov/projects/cmip5/>) (Taylor et al., 2012) database forced by a 1% yr⁻¹ cumulative increase in atmospheric CO₂ concentration (1pctCO₂, named ALL here). These calculations correspond to CO₂ increases from pre-industrial to quadruple pre-industrial levels over 140 years. In addition, we also use two simulations that increase CO₂ either in atmospheric model only (named RAD) or the land surface model only (named PHY). These three simulations allow for the partitioning of changes in each water cycle flux into two components of RAD and PHY. For plant transpiration, the PHY results were further partitioned, offline from the CMIP5 database into the parts caused by stomatal closure (STO) and CO₂ fertilisation on vegetation structure (LAI; see Text S1 in supporting information for details). A limited number of models contributed all of these three simulations to CMIP5 and we use four (CESM1-BGC, IPSL-CM5A-LR, MPI-ESM-LR, and NorESM1-ME; Table S1 in the supporting information) in our analysis, which were selected as they are within ±1 standard deviation of estimated land transpiration to evapotranspiration (T/ET) ratios from isotope observations (Good et al., 2015). The ESMs with realistic values of T/ET may be expected to perform better at simulating future runoff changes (Lian et al., 2018) and biophysical feedbacks (Cui et al., 2020; Zeng et al., 2017). We use ESM diagnostics of monthly CMIP5 output. Model years 1–11 (300 ppm CO₂ on average) and 121–140 (1,034 ppm CO₂) are used to represent the historical and 4×CO₂ climates, respectively (Text S2 in supporting information).

To further validate our results, based on the four models we used with factorial simulations, we adopt for comparison 15 ESMs (Table S2 in the supporting information) in RCP8.5 scenario that have T/ET values falling within one standard deviation of observations (Good et al., 2015). RCP8.5 is selected as in this scenario, CO₂ increases from 378 ppm at 2006 to 936 ppm at the end of 21st century with an average rate of 1% yr⁻¹, which is highly similar to the CO₂ change in ALL simulations by our four main ESMs.

2.2. Definitions of Wetness Gradient and of Wetting Contrast Index (WCI)

To investigate the relationship between the spatial changes of major water fluxes and corresponding wetness levels, we define a background wetness gradient. This gradient is calculated for the historical period (modeled years 1–11), and is the annual mean P-ET (Figure S1 in supporting information). For any particular location, the quantity P-ET is a measure of wetness at that point as it represents the total water availability for land. It can also distinguish between hot wet tropics (e.g., Amazon, central Africa and Maritime Continent) and cold wet northern high latitudes (Figure S1). Across the globe, P-ET generally ranges from 0 to 3 mm day⁻¹ (97% of global land area). We divide global land into 30 bins, based on their P-ET values. Regions with P-ET larger than 3 mm day⁻¹ are not included due to the small fraction of locations this corresponds to. Each bin size is an interval of 0.1 mm day⁻¹. As a sensitivity analysis, we divide global land into other numbers of bins (e.g., 6 bins with an interval of 0.5 mm day⁻¹ and 20 bins with 5% linearly spaced land-area coverage as interval), and obtain similar results (Figure S2 in supporting information). In a further sensitivity check, another wetness index, the ratio of annual precipitation to potential evapotranspiration, P/PET, is used to define wetness gradient and similar results were also found (Figure S2). In the calculation of potential evapotranspiration, we use the Penman-Monteith approach with monthly surface air temperature, relative humidity, surface pressure, latent heat, sensible heat and wind speed as input. Regions within each P-ET bin are kept geographically constant, based on the values for the historical period, in order to isolate changes in water cycle fluxes for different wetness levels (Allan, 2014; Polson & Hegerl, 2017).

To quantify the magnitude of spatial contrast in major water flux changes, we introduce a new summary metric of “Wetting Contrast Index” (WCI). The WCI represents the extent to which the spatial contrast between wet and dry regions, and of the four major land water fluxes, is changing in time. Based on 30 P-ET bins established above and the water cycle flux changes falling within each bin, we calculate a linear regression between them. The slope of ordinary least squares linear regression is defined as the WCI (see schematic diagram Figure S3 and Text S3 in supporting information for details). To demonstrate that the index is not bin number-dependent, we recalculate the linear regression based on all 1°×1° grid cells and corresponding P-ET values across the globe, which returns similar results (Figure S4 in supporting information).

2.3. Wet and Dry Seasons Definitions

We further partition annual land water fluxes changes along wetness gradient into wet and dry seasons. In many locations, seasonal variations have a particularly strong impact on society, and so changes additional to annual mean adjustments require assessment. The wet and dry seasons are defined following the method of Huang et al. (2018), and based on monthly P-ET in the historical period. Monthly anomalies of P-ET are first calculated relative to historical annual mean value. The wet and dry seasons are then defined as P-ET anomalies above and below zero, respectively, in at least two consecutive months. The time periods of the wet and dry seasons are kept constant as modeled CO₂ rises in our study.

3. Results

3.1. Spatial Patterns of Change in Annual Land Water Fluxes

We first investigate the spatial changes in the major water fluxes affecting the land surface. These are changes in precipitation (Δ Precipitation), runoff (Δ Runoff), precipitation minus evapotranspiration (Δ (P-ET)) and evapotranspiration (Δ ET). We find that changes in all four water fluxes, and by the ALL simulations of our four main ESMs analyzed, have strong consistencies with the larger set of projections performed with the broader set of 15 ESMs, as forced by the RCP8.5 scenario (Figures 1a–1d vs. Figures 1e–1h). This consistency indicates that our results are robust despite only four ESMs, with factorial calculations available, forming the bulk of our analysis. In ALL simulations, the annual precipitation, runoff and P-ET all show similar spatial patterns of change in response to rising CO₂ (Figures 1e–1g), whereas changes in ET are smaller (Figure 1h). These changes increase monotonically as CO₂ rises for precipitation, runoff and P-ET and are also generally larger for higher historical P-ET values. In the wet regions, runoff exhibits a broadly uniform increase in increasing values along the wetness gradient, and there is strong consistency on a grid-point (i.e., location) basis. More than 2/3rds of grid-points show consistent sign of change for most wetness and CO₂ levels (hatching in Figure 1f). There are some exceptions, though, with notable heterogeneity

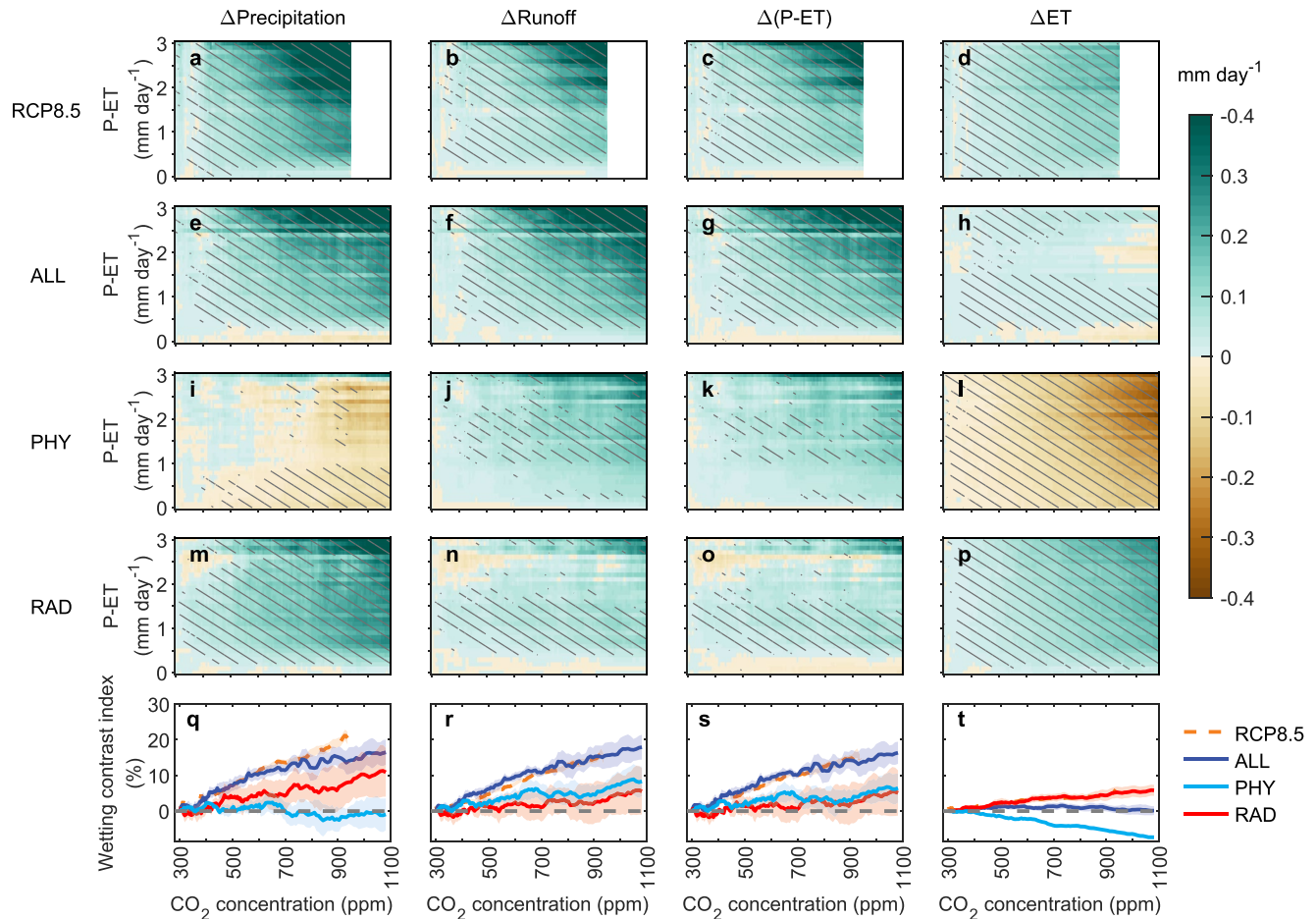


Figure 1. Changes in annual land water fluxes of precipitation, runoff, P-ET and ET. In the top four rows, changes are presented as a function of historical annual P-ET, which defines the wetness gradient (vertical axis; see Methods), and of CO₂ concentration (horizontal axis). Shown are the RCP8.5 scenario ((a–d), 15 ESMs mean changes), then using our four 1pctCO₂ Earth System Models (ESMs), are combined forcing (ALL, (e–h)), and single-forcing simulations of physiological forcing (PHY, (i–l)) and radiative forcing (RAD, (m–p)). The maximum CO₂ concentration in the RCP8.5 scenario is 936 ppm (a–d). Hatching indicates where >67% of the grid-boxes agree on the sign of change in each wetness-CO₂ bin. Bottom row, (q–t), are WCIs calculated for precipitation change (q), runoff change (r), P-ET change (s) and ET change (t), respectively. The shaded areas in panels (q–t) represent the standard errors of the mean of the four ESMs.

among different wet regions at 4×CO₂ concentration (Figure S5 in supporting information). Tropical Africa and Maritime Continent are projected to have substantial runoff increases, whereas runoff decreases in northeast Amazonia despite having a similar background wetness level.

In dry regions, although the magnitude of the change is less than that in wet regions, annual precipitation, runoff and P-ET do also increase with rising atmospheric CO₂, challenging the WWDD concept. The exception to this is for extremely dry regions which have a slight decrease in precipitation, P-ET and ET (Figures 1e, 1g and 1h). Furthermore, changes in the three water fluxes all show non-uniform spatial patterns in dry regions, as shown by the wetness levels close to zero with no hatching in Figures 1e–1g. In particular, in Australia, runoff is projected to increase at 4×CO₂ concentration, while it instead decreases in the dry southwest North America and West Asia (Figure S5 in supporting information). These very dry regions are, though, anomalies, and it is notable that even for relatively dry regions (i.e., low historical P-ET), the terrestrial water fluxes actually increase.

Overall, precipitation, runoff and P-ET all exhibit a general increasing tendency as CO₂ levels rise. In addition, the amount of wetting is generally larger in wet regions, where background P-ET is larger, compared to dry regions. As a consequence, the contrast of these three water fluxes between wet and dry regions strengthens substantially (Figures 1e–1g) as CO₂ rises. To quantify the magnitude of this contrast,

we calculate our metric of WCI. We find that all three water flux-based WCIs increase nearly linearly with increasing atmospheric CO_2 , at a rate of approximately $3\% \text{ mm day}^{-1}$ (mm day^{-1}) per 100 ppm increase in CO_2 relative to historical period (Figures 1q–1s; dark blue lines). This rate of increase is also supported by WCIs based on changes by 15 ESMS forced by atmospheric greenhouse gas concentrations following the RCP8.5 scenario (brown dashed line in Figures 1q–1s). For the runoff-based WCI, it attains a value of 18% at $4\times\text{CO}_2$. Hence for two places, where the second one has a background historical runoff that is, 1.0 mm day^{-1} higher than the first, then at $4\times\text{CO}_2$, the second location can be expected to have a rise in runoff that is, 0.18 mm day^{-1} larger than the first. In contrast, ET-based WCI increases more slowly as CO_2 levels rise (dark blue line in Figure 1t). Additional analyses reinforce that larger water flux changes along the wetness gradient are robust, regardless of which wetness index or bin interval is used (Figure S2 in supporting information). Our results quantitatively confirm that a considerable amplification of land water fluxes contrast between wet and dry regions will emerge under a high emissions scenario.

3.2. Dominant Drivers of Change in Annual Land Water Fluxes

We further find that the driving factors are different among the four water fluxes (Figures 1i–1p). For precipitation, and spanning the full range of atmospheric CO_2 concentrations, RAD forcing dominates the overall increase along the wetness gradient (Figure 1m vs. Figure 1i). The PHY influence on precipitation is not negligible though, and Figure 1i provides a direct illustration of how the land surface can feedback to modulate rainfall across wetness and CO_2 levels. In contrast to precipitation, PHY forcings shift runoff and P-ET in both wet and dry regions towards a general wetting. Such wetting is due to major evapotranspiration reduction, and again these flux changes are larger in wet regions than those in dry regions (Figures 1j–1l). Although the impacts of RAD on runoff and P-ET changes are comparable to that of PHY, PHY forcings pose a slightly larger impact on the increases in these two water fluxes, especially for runoff (Figures 1j and 1k vs. Figures 1n–1o). It can be noted that runoff and P-ET changes show less regional consistency in each wetness- CO_2 bin in both PHY and RAD forcings than in ALL forcings (hatching in Figures 1j and 1k and 1n–1o vs. more extensive hatching in Figure 1f–1g). These forcings all contribute to driving the contrasting changes between wet and dry regions for runoff and P-ET. In summary, RAD-driven precipitation increases and PHY-induced ET reductions (which compensates the RAD-driven tendency to increase ET), lead to overall large runoff increases, which are strongest in historically wet regions, in the ALL forcings simulations.

Figure 1q–t shows the WCI contributions for RAD and PHY forcings, in the red and light blue curves respectively. RAD dominates the increase in precipitation-based WCI with increasing CO_2 , whereas PHY drives larger (or comparable) increases in runoff- and P-ET-based WCIs due to an offsetting reduction in ET (Figure 1t). However, there is larger spread across the four models for the impacts of these two forcings on runoff and P-ET-based WCIs. Specifically, at $4\times\text{CO}_2$ concentration, the ratios of WCI between PHY and RAD for runoff are 1.6 (WCI: 8.2% for PHY and 5.1% for RAD) and for P-ET changes are 1.3 (6.2% and 4.9%) (compare years 121–140 of light blue and red curves; Figures 1r–1s). For ET-based WCI, the impacts of RAD and PHY are opposite and comparable, and largely cancel each other out (Figure 1t). The light blue curves of Figures 1r–1t verify the critical importance of PHY forcing in reshaping the distribution of land water fluxes change across wetness levels.

Figure 1 shows how both PHY and RAD forcings operate on the terrestrial water cycle as a function of background wetness gradient and CO_2 changing levels. In Figure 2, we present which of these two forcings contributes the most to the main water fluxes at the regional scale. The dominant drivers for precipitation, runoff and P-ET changes show large latitudinal differences, and where such variation also changes as CO_2 levels rise (Figures 2a, 2c and 2e). At CO_2 levels below ~ 500 ppm, there is no zonally uniform dominant driver in any of the three water fluxes. However, as atmospheric CO_2 levels rise, RAD generally dominates precipitation change over most latitudinal averages, except the regions near 30°N or 30°S (Figure 2a). For both runoff and P-ET, PHY tends to progressively extend, latitudinally, its dominance on the changes in tropical and temperate regions in response to rising CO_2 (Figures 2c and 2e). Notable is that PHY has a larger contribution to the change than RAD for 28%, 40% and 40% of global land surface for precipitation, runoff and P-ET changes at $4\times\text{CO}_2$ concentration, respectively (green areas in Figures 2b, 2d and 2f). In general, these locations correspond to stomatal closure-induced ET reduction (Figures 2h and S6 in supporting

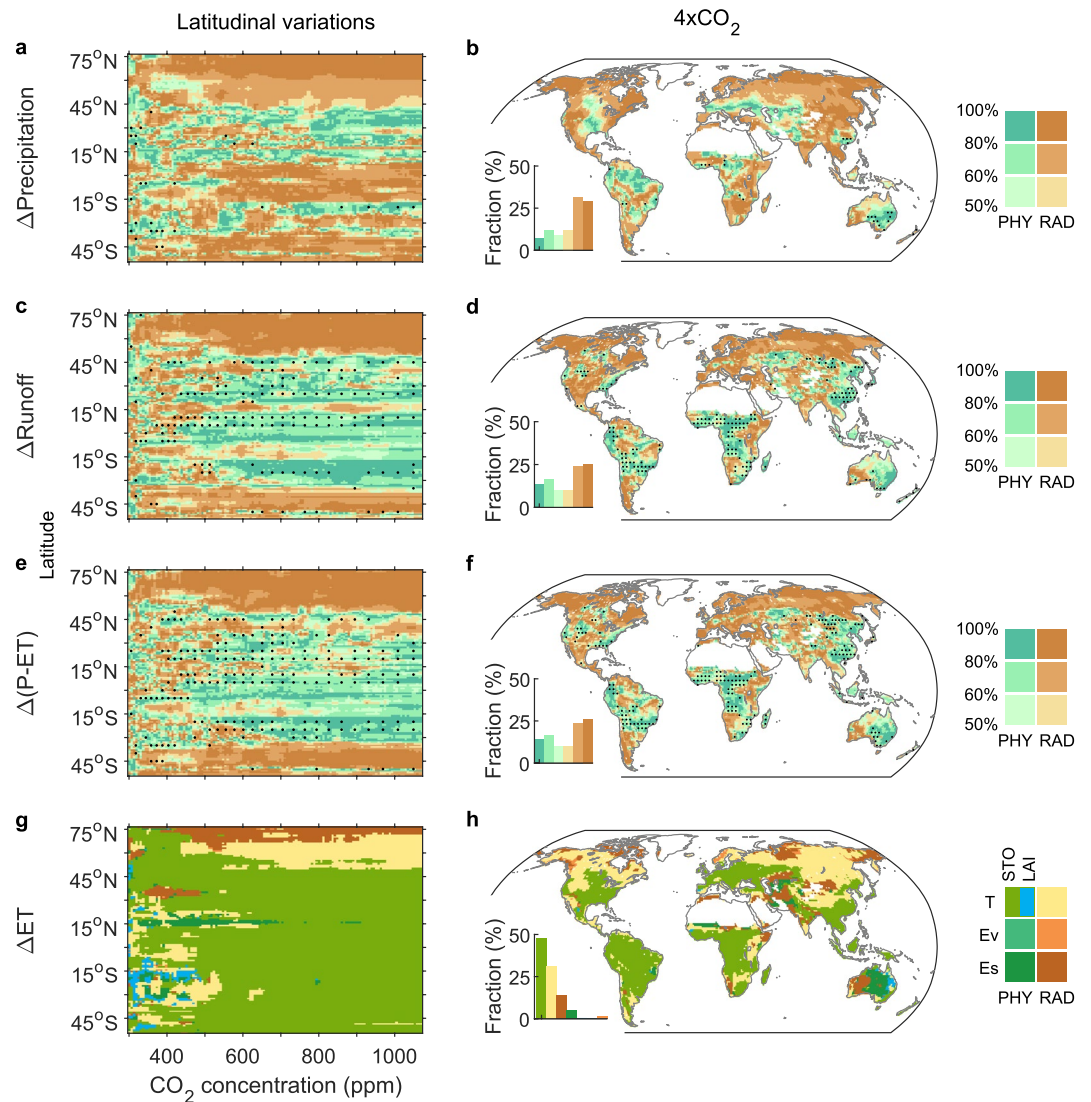


Figure 2. The dominant spatiotemporal drivers of changes to land water fluxes, and their magnitude of contribution. Dominant drivers are defined as the driving factor that contributes the most to the increase (or decrease) in each water flux in each vegetated grid cell. For precipitation, runoff and P-ET changes, the dominant driver is further divided into three levels according to the driver's percentage contribution to total water flux changes (bounds of 50%–60%, 60%–80% and 80%–100%). The ET flux is further partitioned into whether transpiration (T), soil evaporation (Es) or vegetation canopy evaporation (Ev) changes dominate (but without their percentage influence). The PHY forcing of transpiration is further partitioned into either stomatal closure (STO) and CO₂ fertilisation that is, LAI changes (see Methods). In panel (a–f), stippling indicates regions where the PHY-driven water flux increase has a larger magnitude than RAD-driven component decrease, so the combined impact is an increase. A frequency distribution of the dominant drivers is shown in the insets at the bottom-left for each global map, using identical colors to those in the main plot of each panel.

information) (Skinner et al., 2017). Although these percentages are less than 50%, this result is not inconsistent with PHY having a larger (or comparable) contribution than RAD to the WCI values for runoff and P-ET. PHY shifts both wet and dry regions toward general wetting, and further, the magnitude of increase in wet regions is larger than that in dry regions (Figures 1j and 1k). The rates of increase in RAD are less correlated with wetness gradient than PHY (Figures 1n–1o), making RAD have a more secondary role in driving the overall amplification of the runoff and P-ET contrasts, as captured in our WCI metric (Figures 1r–1s). Comparatively, the dominant drivers are distinct among different dry regions (Figures 2b, 2d and 2f). In eastern Australia and the Sahel, the three water fluxes (precipitation, runoff and P-ET) are all dominated by

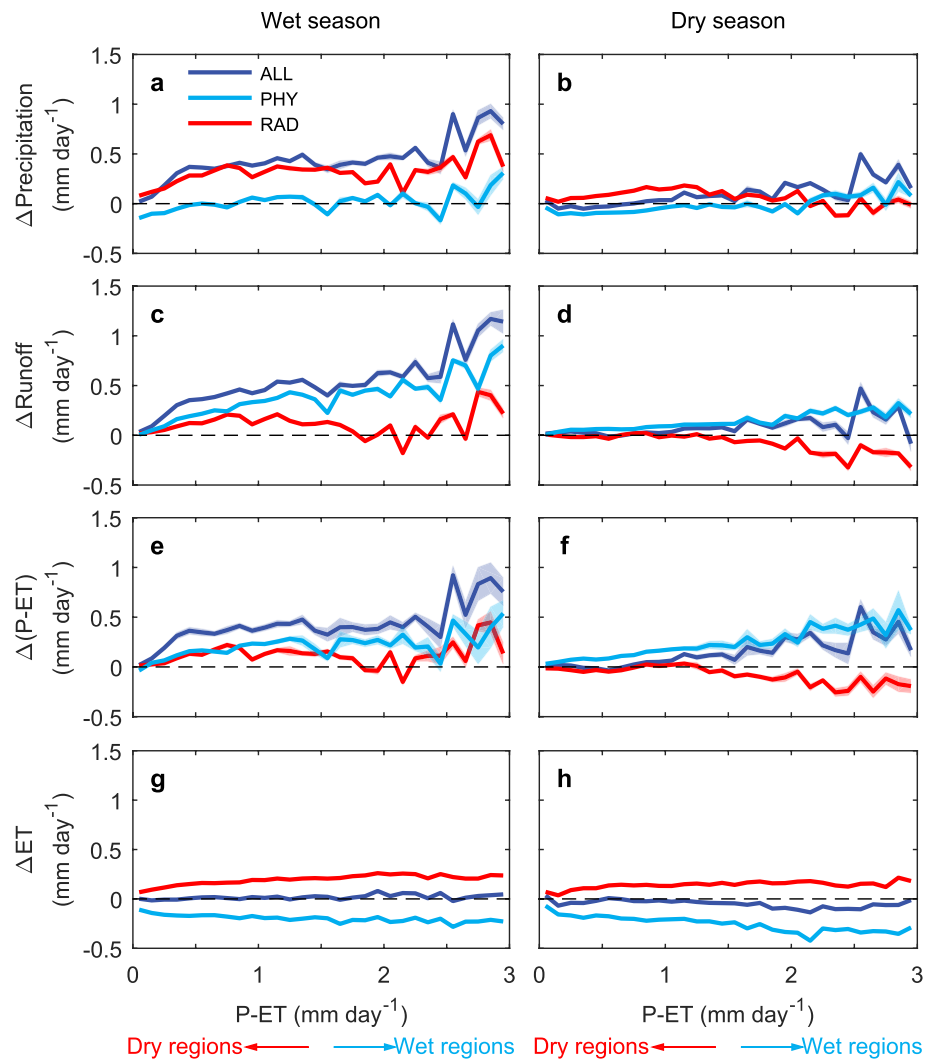


Figure 3. Changes in land water fluxes for different background wetness levels, and in both wet and dry seasons for different forcings at $4\times\text{CO}_2$ concentration. The simulations are for ALL, PHY and RAD configurations of Earth System Models (ESMs). The shaded areas represent standard errors of the four ESMs used.

PHY. However, they are all generally controlled by RAD over other dry regions, including southwest North America, south Africa and South America.

Of particular interest is that the PHY-driven runoff increase has a larger magnitude than RAD-induced runoff decrease in 15% of global land area at $4\times\text{CO}_2$ concentration, including the Sahel, central Africa, southern China, western and southern Amazonia (stippling in Figure 2d). This finding implies that the CO_2 -induced PHY effect is stronger than the opposing increased evaporative demand from RAD caused directly by radiative warming. For these regions, which include some arid regions, this balance suggests more freshwater resources as CO_2 rises.

3.3. Land Water Flux Changes in Wet and Dry Seasons

To explore the seasonal contribution to the strengthening contrast in forcings between wet and dry regions, we investigate the three water fluxes changes along the wetness gradient for $4\times\text{CO}_2$, and now disaggregated to both wet and dry seasons (Figure 3). We find that it is water flux changes in wet seasons that mainly contribute the contrasting changes in annual precipitation (64% of annual WCI), runoff (83%) and P-ET (55%), again presented along the wetness gradient. The magnitude of increase ($0.5\text{--}1.2\text{ mm day}^{-1}$) is particularly

strong at wetness levels above 2 mm day^{-1} , leading up to about 50% more water resources (Figures 3c and 3e) being available in these very wet regions. In the dry season, however, the changes in the three water fluxes are much less than that in wet seasons, although the contrast of changes between wet and dry regions remain, as shown by the positive gradient of the dark blue lines in Figures 3b, 3d and 3f.

For the seasonal effects of the single forcing, we find that in the wet season, RAD dominates the amplification of precipitation contrast between wet and dry regions (red line in Figure 3a). However, notable is that PHY feedbacks play a role by increasing precipitation overall in extremely wet regions (highest P-ET values, light blue curve, Figure 3a). PHY substantially strengthens runoff and P-ET contrast between wet and dry regions, and unlike for precipitation, with a larger contribution than RAD for runoff and similar for P-ET (light blue lines in Figures 3c–3f). Runoff and P-ET increase under PHY forcing across all wetness levels in both seasons, and with the most substantial changes in the wettest locations, thereby in support of WCI-based results at seasonal timescales. Of particular interest is that in the dry season, the RAD forcing lowers runoff and P-ET for high wetness levels, but these changes are overcome by larger PHY forcings (Figures 3d and 3f). This finding indicates that overall the vegetation response to rising CO_2 may alleviate dry-season water stress in these regions despite continuous global warming. Overall, our results indicate that the PHY forcing dominates the strengthening contrast of land water resources between wet and dry regions, especially by enhancing runoff in the wet season and countering the effects of RAD in the dry season.

4. Discussion

By assessing the main terrestrial hydrological changes along a continuous wetness gradient, we find that land water resources increase for both wet and dry regions in response to rising CO_2 , except for some very dry regions. In this context, our results are not consistent with the previously suggested WWDD paradigm (Chou et al., 2009; Held & Soden, 2006), and in particular the “dry regions get drier” component. However, we do find some similarity, in the sense that the wet regions do get wetter (Kumar et al., 2015; Polson & Hegerl, 2017). The WWDD paradigm is frequently proposed to depict the zonally averaged large-scale changes in P-ET (Held & Soden, 2006). We, therefore, perform similar assessments by analyzing the changes in P-ET, as well as for precipitation and runoff, presented as the land zonal-means (Figure S7 in supporting information). We find that all three water fluxes substantially increase in the tropics and northern high latitudes. However, we also find evidence of smaller but still increasing fluxes in the drier subtropics (Figure S7), again challenging the WWDD paradigm. Furthermore, in previous assessments of WWDD (Greve et al., 2014; Greve & Seneviratne, 2015; Kumar et al., 2015; Polson & Hegerl, 2017; T. Yang et al., 2019), the land is usually divided into either “wet regions” or “dry regions” using a specific threshold of an aridity index. An example index value might be 2.0 for the ratio of potential evapotranspiration to precipitation (i.e., PET/P). However, the land consists of regions with a broad range of background wetness or aridity levels. Hence our continuum-based WCI framework can provide more information across the spectrum of such wetness and thus improve the assessment of terrestrial hydrological cycle changes.

Although land water resources are projected to increase in both wet and dry regions as CO_2 rise, the magnitude of increase in wet regions is much larger than that in dry regions, and as characterized with our WCI metric. Our results indicate that this amplifying contrast, for runoff (and P-ET), is mainly driven by vegetation CO_2 physiological forcing (Figures 1r–1s). Physiological CO_2 -driven forcing influences global land water cycles largely through two opposing effects: stomatal closure, which reduces transpiration (Field et al., 1995; Morison & Gifford, 1983) and the CO_2 fertilisation effect that induces LAI expansion, which increases transpiration (Cowling & Field, 2003; Piao et al., 2007). Hence, we further analyze the impacts of stomatal closure and LAI increase on plant transpiration in regions with different wetness levels. In general, in wet regions, vegetation cover is expected to reach saturation as CO_2 rises, as the fertilisation effect becomes limited by light, temperature and nutrient availability (Norby & Zak, 2011; Ukkola et al., 2015). However, CO_2 -induced stomatal closure continues as CO_2 rises, with less evidence of saturation than LAI (Maherali et al., 2002). Hence the overall PHY forcings become dominated by stomatal closure over LAI increase, and as we confirm in our simulations (Figures S8b–S8d in supporting information) and also in a previous coupled land-atmosphere separation simulation (Skinner et al., 2017). As a consequence, transpiration reduction conserves and thus increases land water resources in wet regions (e.g., central Africa and Maritime Continent; Figures S5b and S5c). In dry regions, vegetation cover is generally more sparse, and

rising CO₂ causes greater relative plant growth, with associated LAI increase (Donohue et al., 2013; Fatichi et al., 2016; Morgan et al., 2011) (Figure S8a). Hence, in drier locations, LAI-induced transpiration increase offsets a more substantial fraction of transpiration reduction from stomatal closure (Figures S8b–S8c) (Lian et al., 2021; Trancoso et al., 2017; Ukkola et al., 2015). Overall, this balance in dry regions still results in increases in runoff and P-ET (e.g., Sahel and Australia; Figures S5b and S5c), but the amount is much less than for wet regions. It is this different trade-off between stomatal closure and LAI increase that accounts for the larger amplification of land water resources in wet regions, and as represented in our PHY-based WCI values.

5. Conclusions

In summary, our results show that more water resources are projected to be available over land in response to rising CO₂ in both wet and dry regions, although some regional heterogeneity may exist between locations within the same wetness levels. However, there is a contrast of land water resource changes between wet and dry regions, and that will strengthen markedly as CO₂ increases. We quantify this contrast by our new Wetting Contrast Index (WCI), which shows the stronger increases in wet regions of land water resources. Such increases are mainly driven by vegetation-physiological forcing, although radiatively driven climate change also plays an important role in these increases. Hence to further refine estimates of expected change to future water availability, we encourage the on-going refinement of modeled responses of stomatal conductance and LAI to rising CO₂. This priority for research will be supported by the emerging controlled field experiments that will further constrain our understanding of the hydrological impacts of plants in response to rising CO₂, such as the free-air CO₂ enrichment experiments (Norby & Zak, 2011), and especially the new locations in extreme wet (e.g., Amazonia) and dry regions. Although vegetation physiology increases land water resources with higher CO₂, which may alleviate drought stress for humans and ecosystems in dry regions, it has the potential to exacerbate the risks of regional extreme flooding events. However, our noted changes are mean responses to rising CO₂, and changes in extremes such as floods and droughts are also driven by change in variability (e.g., Ukkola et al., 2020). Of particular interest is that our study also highlights that vegetation-rainfall feedbacks play a critical role in reshaping the future spatial distribution of global land water resources. Our findings provide beneficial information for water cycle projections and water resource management, aiding policymakers to evaluate the expected impacts of climate change on continental water resources. Yet despite finding a diverse range of potential responses, we find a substantial ability to reduce such complexity, and in particular through mapping changes on to our simple but informative WCI metric.

Data Availability Statement

All data sets and materials used in this study are freely available online: <https://esgf-node.llnl.gov/projects/cmip5/> (Taylor et al., 2012). The codes used in our analyses are available on repository (https://figshare.com/articles/software/Codes_for_WWDD_paper_on_GRL/14562033).

References

- Ainsworth, E. A., & Long, S. P. (2005). What have we learned from 15 years of free-air CO₂ enrichment (FACE)? A meta-analytic review of the responses of photosynthesis, canopy properties and plant production to rising CO₂. *New Phytologist*, *165*(2), 351–372. <https://doi.org/10.1111/j.1469-8137.2004.01224.x>
- Ainsworth, E. A., & Rogers, A. (2007). The response of photosynthesis and stomatal conductance to rising [CO₂]: Mechanisms and environmental interactions. *Plant, Cell and Environment*, *30*(3), 258–270. <https://doi.org/10.1111/j.1365-3040.2007.01641.x>
- Allan, R. P. (2014). Dichotomy of drought and deluge. *Nature Geoscience*, *7*, 700–701. <https://doi.org/10.1038/ngeo2243>
- Allan, R. P., Barlow, M., Byrne, M. P., Cherchi, A., Douville, H., Fowler, H. J., et al. (2020). Advances in understanding large-scale responses of the water cycle to climate change. *Proceedings of the National Academy of Sciences*, *147*(1), 49–75. <https://doi.org/10.1111/nyas.14337>
- Betts, R. A., Boucher, O., Collins, M., Cox, P. M., Falloon, P. D., Gedney, N., et al. (2007). Projected increase in continental runoff due to plant responses to increasing carbon dioxide. *Nature*, *448*(7157), 1037–1041. <https://doi.org/10.1038/nature06045>
- Byrne, M. P., & O’Gorman, P. A. (2015). The response of precipitation minus evapotranspiration to climate warming: Why the “Wet-get-wetter, dry-get-drier” scaling does not hold over land. *Journal of Climate*, *28*(20), 8078–8092. <https://doi.org/10.1175/jcli-d-15-0369.1>
- Cao, L., Bala, G., Caldeira, K., Nemani, R., & Ban-Weiss, G. (2010). Importance of carbon dioxide physiological forcing to future climate change. *Proceedings of the National Academy of Sciences of the United States of America*, *107*(21), 9513–9518. <https://doi.org/10.1073/pnas.0913000107>

Acknowledgments

This study was supported by the National Natural Science Foundation of China (41988101). Chris Huntingford was supported by the Newton Fund through the Met Office Climate Science for Service Partnership China (CSSP China). GJK acknowledges support from the U.S. Department of Energy (DOE) and Regional and Global Model Analysis (RGMA) Program (DE-SC0019459 and DE-SC0021209). We thank the four ESM modeling groups that provided the single-forcing simulations: National Science Foundation, Department of Energy, National Center for Atmospheric Research (CESM1-BGC), Institut Pierre-Simon Laplace (IPSL-CM5A-LR), Max Planck Institute for Meteorology (MPI-ESM-LR) and Norwegian Climate Centre (NorESM1-ME). The authors also thank Philippe Ciais for improving earlier version of the manuscript.

- Chadwick, R., Boutle, I., & Martin, G. (2013). Spatial patterns of precipitation change in CMIP5: Why the rich do not get richer in the tropics. *Journal of Climate*, 26(11), 3803–3822. <https://doi.org/10.1175/jcli-d-12-00543.1>
- Chou, C., Neelin, J. D., Chen, C.-A., & Tu, J.-Y. (2009). Evaluating the “rich-get-richer” mechanism in tropical precipitation change under global warming. *Journal of Climate*, 22(8), 1982–2005. <https://doi.org/10.1175/2008jcli2471.1>
- Cowling, S. A., & Field, C. B. (2003). Environmental control of leaf area production: Implications for vegetation and land-surface modeling. *Global Biogeochemical Cycles*, 17(1), 7–17. <https://doi.org/10.1029/2002gb001915>
- Cui, J., Piao, S., Huntingford, C., Wang, X., Lian, X., Chevuturi, A., et al. (2020). Vegetation forcing modulates global land monsoon and water resources in a CO₂-enriched climate. *Nature Communications*, 11(1), 5184. <https://doi.org/10.1038/s41467-020-18992-7>
- De Kauwe, M. G., Medlyn, B. E., Zaehle, S., Walker, A. P., Dietze, M. C., Hickler, T., et al. (2013). Forest water use and water use efficiency at elevated CO₂: A model-data intercomparison at two contrasting temperate forest FACE sites. *Global Change Biology*, 19(6), 1759–1779. <https://doi.org/10.1111/gcb.12164>
- Donohue, R. J., Roderick, M. L., McVicar, T. R., & Farquhar, G. D. (2013). Impact of CO₂ fertilization on maximum foliage cover across the globe's warm, arid environments. *Geophysical Research Letters*, 40(12), 3031–3035. <https://doi.org/10.1002/grl.50563>
- Durack, P. J., Wijffels, S. E., & Matear, R. J. (2012). Ocean salinities reveal strong global water cycle intensification during 1950 to 2000. *Science*, 336(6080), 455–458. <https://doi.org/10.1126/science.1212222>
- Fatichi, S., Leuzinger, S., Paschalis, A., Langley, J. A., Donnellan Barraclough, A., & Hovenden, M. J. (2016). Partitioning direct and indirect effects reveals the response of water-limited ecosystems to elevated CO₂. *Proceedings of the National Academy of Sciences of the United States of America*, 113(45), 12757–12762. <https://doi.org/10.1073/pnas.1605036113>
- Field, C. B., & Jackson, R. B., & Mooney, H. A. (1995). Stomatal responses to increased CO₂: Implications from the plant to the global scale. *Plant, Cell and Environment*, 18(10), 1214–1225. <https://doi.org/10.1111/j.1365-3040.1995.tb00630.x>
- Fowler, M. D., Kooperman, G. J., Randerson, J. T., & Pritchard, M. S. (2019). The effect of plant physiological responses to rising CO₂ on global streamflow. *Nature Climate Change*, 9(11), 873–879. <https://doi.org/10.1038/s41558-019-0602-x>
- Gedney, N., Cox, P. M., Betts, R. A., Boucher, O., Huntingford, C., & Stott, P. A. (2006). Detection of a direct carbon dioxide effect in continental river runoff records. *Nature*, 439(7078), 835–838. <https://doi.org/10.1038/nature04504>
- Good, S. P., Noone, D., & Bowen, G. (2015). Hydrologic connectivity constrains partitioning of global terrestrial water fluxes. *Science*, 349(6244), 175–177. <https://doi.org/10.1126/science.aaa5931>
- Greve, P., Orlovsky, B., Mueller, B., Sheffield, J., Reichstein, M., & Seneviratne, S. I. (2014). Global assessment of trends in wetting and drying over land. *Nature Geoscience*, 7(10), 716–721. <https://doi.org/10.1038/ngeo2247>
- Greve, P., & Seneviratne, S. I. (2015). Assessment of future changes in water availability and aridity. *Geophysical Research Letters*, 42(13), 5493–5499. <https://doi.org/10.1002/2015gl064127>
- Held, I. M., & Soden, B. J. (2006). Robust responses of the hydrological cycle to global warming. *Journal of Climate*, 19(21), 5686–5699. <https://doi.org/10.1175/jcli3990.1>
- Huang, M., Wang, X., Keenan, T. F., & Piao, S. (2018). Drought timing influences the legacy of tree growth recovery. *Global Change Biology*, 24(8), 3546–3559. <https://doi.org/10.1111/gcb.14294>
- IPCC. (2013). *Climate change 2013: The physical science basis. Contribution of working group I to the fifth assessment report of the intergovernmental panel on climate change*. In T. Stocker, D. Qin, G. Plattner, M. Tignor, S. Allen, J. Boschung, A. Nauels, Y. Xia, B. Bex, & B. Midgley (Eds.), Cambridge University Press.
- Kooperman, G. J., Chen, Y., Hoffman, F. M., Koven, C. D., Lindsay, K., Pritchard, M. S., et al. (2018). Forest response to rising CO₂ drives zonally asymmetric rainfall change over tropical land. *Nature Climate Change*, 8(5), 434–440. <https://doi.org/10.1038/s41558-018-0144-7>
- Kumar, S., Allan, R. P., Zwiers, F., Lawrence, D. M., Dirmeyer, P. A. (2015). Revisiting trends in wetness and dryness in the presence of internal climate variability and water limitations over land. *Geophysical Research Letters*, 42(24), 10867–10875. <https://doi.org/10.1002/2015GL066858>
- Lemordant, L., Gentine, P., Swann, A. S., Cook, B. I., & Scheff, J. (2018). Critical impact of vegetation physiology on the continental hydrologic cycle in response to increasing CO₂. *Proceedings of the National Academy of Sciences*, 115(16), 4093–4098. <https://doi.org/10.1073/pnas.1720712115>
- Lian, X., Piao, S., Chen, A., Huntingford, C., Fu, B., Li, L. Z. X., et al. (2021). Multifaceted characteristics of dryland aridity changes in a warming world. *Nature Reviews Earth & Environment*, 2, 232–250. <https://doi.org/10.1038/s43017-021-00144-0>
- Lian, X., Piao, S., Huntingford, C., Li, Y., Zeng, Z., Wang, X., et al. (2018). Partitioning global land evapotranspiration using CMIP5 models constrained by observations. *Nature Climate Change*, 8(7), 640–646. <https://doi.org/10.1038/s41558-018-0207-9>
- Liu, C., & Allan, R. P. (2013). Observed and simulated precipitation responses in wet and dry regions 1850–2100. *Environmental Research Letters*, 8(3), 034002. <https://doi.org/10.1088/1748-9326/8/3/034002>
- Maherali, H., Reid, C. D., Polley, H. W., Johnson, H. B., & Jackson, R. B. (2002). Stomatal acclimation over a subambient to elevated CO₂ gradient in a C-3/C-4 grassland. *Plant, Cell and Environment*, 25(4), 557–566. <https://doi.org/10.1046/j.1365-3040.2002.00832.x>
- Mankin, J. S., Seager, R., Smerdon, J. E., Cook, B. I., & Williams, A. P. (2019). Mid-latitude freshwater availability reduced by projected vegetation responses to climate change. *Nature Geoscience*, 12(12), 983–988. <https://doi.org/10.1038/s41561-019-0480-x>
- Milly, P. C. D., & Dunne, K. A. (2016). Potential evapotranspiration and continental drying. *Nature Climate Change*, 6, 946–949. <https://doi.org/10.1038/nclimate3046>
- Morgan, J. A., LeCain, D. R., Pendall, E., Blumenthal, D. M., Kimball, B. A., Carrillo, Y., et al. (2011). C4 grasses prosper as carbon dioxide eliminates desiccation in warmed semi-arid grassland. *Nature*, 476(7359), 202–205. <https://doi.org/10.1038/nature10274>
- Morison, J. I. L., & Gifford, R. M. (1983). Stomatal sensitivity to carbon dioxide and humidity. *Plant Physiology*, 71(4), 789–796. <https://doi.org/10.1104/pp.71.4.789>
- Norby, R. J., & Zak, D. R. (2011). Ecological lessons from free-air CO₂ enrichment (FACE) experiments. *Annual Review of Ecology and Systematics*, 42(1), 181–203. <https://doi.org/10.1146/annurev-ecolsys-102209-144647>
- Piao, S., Friedlingstein, P., Ciais, P., de Noblet-Ducoudre, N., Labat, D., & Zaehle, S. (2007). Changes in climate and land use have a larger direct impact than rising CO₂ on global river runoff trends. *Proceedings of the National Academy of Sciences of the United States of America*, 104(39), 15242–15247. <https://doi.org/10.1073/pnas.0707213104>
- Piao, S., Wang, X., Park, T., Chen, C., Lian, X., He, Y., et al. (2020). Characteristics, drivers and feedbacks of global greening. *Nature Reviews Earth & Environment*, 1(1), 14–27. <https://doi.org/10.1038/s43017-019-0001-x>
- Polson, D., & Hegerl, G. C. (2017). Strengthening contrast between precipitation in tropical wet and dry regions. *Geophysical Research Letters*, 44(1), 365–373. <https://doi.org/10.1002/2016gl071194>
- Pu, B., & Dickinson, R. E. (2014). Hydrological changes in the climate system from leaf responses to increasing CO₂. *Climate Dynamics*, 42(7), 1905–1923. <https://doi.org/10.1007/s00382-013-1781-1>

- Roderick, M. L., Sun, F., Lim, W. H., & Farquhar, G. D. (2014). A general framework for understanding the response of the water cycle to global warming over land and ocean. *Hydrology and Earth System Sciences*, 18(5), 1575–1589. <https://doi.org/10.5194/hess-18-1575-2014>
- Scheff, J., Mankin, S. J., Coats, S., & Liu, H. (2021). CO₂-plant effects do not account for the gap between dryness indices and projected dryness impacts in CMIP6 or CMIP5. *Environmental Research Letters*, 16(3), 034018. <https://doi.org/10.1088/1748-9326/abd8fd>
- Seager, R., & Vecchi, G. A. (2010). Greenhouse warming and the 21st century hydroclimate of southwestern North America. *Proceedings of the National Academy of Sciences of the United States of America*, 107(50), 21277–21282. <https://doi.org/10.1073/pnas.0910856107>
- Seneviratne, S. I., Corti, T., Davin, E. L., Hirschi, M., Jaeger, E. B., Lehner, I., et al. (2010). Investigating soil moisture–climate interactions in a changing climate: A review. *Earth-Science Reviews*, 99(3), 125–161. <https://doi.org/10.1016/j.earscirev.2010.02.004>
- Skinner, C. B., Poulsen, C. J., Chadwick, R., Diffenbaugh, N. S., & Fiorella, R. P. (2017). The role of plant CO₂ physiological forcing in shaping future daily-scale precipitation. *Journal of Climate*, 30(7), 2319–2340. <https://doi.org/10.1175/jcli-d-16-0603.1>
- Swann, A. L., Hoffman, F. M., Koven, C. D., & Randerson, J. T. (2016). Plant responses to increasing CO₂ reduce estimates of climate impacts on drought severity. *Proceedings of the National Academy of Sciences of the United States of America*, 113(36), 10019–10024. <https://doi.org/10.1073/pnas.1604581113>
- Taylor, K. E., Stouffer, R. J., & Meehl, G. A. (2012). An overview of CMIP5 and the experiment design. *Bulletin of the American Meteorological Society*, 93(4), 485–498. <https://doi.org/10.1175/bams-d-11-00094.1>
- Trancoso, R., Larsen, J. R., McVicar, T. R., Phinn, S. R., & McAlpine, C. A. (2017). CO₂-vegetation feedbacks and other climate changes implicated in reducing base flow. *Geophysical Research Letters*, 44(5), 2310–2318. <https://doi.org/10.1002/2017gl072759>
- Trenberth, K. E. (2011). Changes in precipitation with climate change. *Climate Research*, 47(1), 123–138. <https://doi.org/10.3354/cr00953>
- Ukkola, A. M., De Kauwe, M. G., Roderick, M. L., Abramowitz, G., & Pitman, A. J. (2020). Robust future changes in meteorological drought in CMIP6 projections despite uncertainty in precipitation. *Geophysical Research Letters*, 47(11). <https://doi.org/10.1029/2020gl087820>
- Ukkola, A. M., Prentice, I. C., Keenan, T. F., van Dijk, A. I. J. M., Viney, N. R., Myneni Ranga, B., & Bi, J. (2015). Reduced streamflow in water-stressed climates consistent with CO₂ effects on vegetation. *Nature Climate Change*, 6(1), 75–78. <https://doi.org/10.1038/nclimate2831>
- Yang, T., Ding, J., Liu, D., Wang, X., & Wang, T. (2019). Combined use of multiple drought indices for global assessment of dry gets drier and wet gets wetter paradigm. *Journal of Climate*, 32(3), 737–748. <https://doi.org/10.1175/jcli-d-18-0261.1>
- Yang, Y., Donohue, R. J., McVicar, T. R., Roderick, M. L., & Beck, H. E. (2016). Long-term CO₂ fertilization increases vegetation productivity and has little effect on hydrological partitioning in tropical rainforests. *Journal of Geophysical Research: Biogeosciences*, 121(8), 2125–2140. <https://doi.org/10.1002/2016jg003475>
- Yang, Y., Roderick, M. L., Zhang, S., McVicar, T. R., & Donohue, R. J. (2019). Hydrologic implications of vegetation response to elevated CO₂ in climate projections. *Nature Climate Change*, 9(1), 44–48. <https://doi.org/10.1038/s41558-018-0361-0>
- Zeng, Z., Piao, S., Li, L. Z. X., Zhou, L., Ciais, P., Wang, T., et al. (2017). Climate mitigation from vegetation biophysical feedbacks during the past three decades. *Nature Climate Change*, 7(6), 432–436. <https://doi.org/10.1038/nclimate3299>
- Zhu, Z., Piao, S., Myneni, R. B., Huang, M., Zeng, Z., Canadell, J. G., et al. (2016). Greening of the Earth and its drivers. *Nature Climate Change*, 6(8), 791–795. <https://doi.org/10.1038/nclimate3004>